

INSPIRALING DOUBLE COMPACT OBJECT DETECTION AND LENSING RATE – FORECAST FOR DECIGO AND B-DECIGO

ALEKSANDRA PIÓRKOWSKA-KURPAS^{1,2}, SHAOQI HOU³, MAREK BIESIADA^{1,4}, XUHENG DING^{3,5}, SHUO CAO^{1*}, XILONG FAN^{3†},
SEIJI KAWAMURA⁶ AND ZONG-HONG ZHU^{1,3}

Draft version November 9, 2021

ABSTRACT

Emergence of gravitational wave (GW) astronomy revived the interest in exploring the low frequency GW spectrum inaccessible from the ground. Satellite GW observatory DECIGO in its original configuration and the currently proposed smaller scale B-DECIGO are aimed to cover deci-Hertz part of the GW spectrum, which fills the gap between LISA mili-Hertz and deca- to kilo-Hertz range probed by ground-based detectors. In this paper we forecast the detection rates of inspiraling double compact objects (DCOs) and the unresolved confusion noise from these sources in DECIGO and B-DECIGO. In the context of DECIGO we use, for the first time, the population synthesis intrinsic inspiral rates of NS-NS, BH-NS and BH-BH systems. We also estimate the expected gravitational lensing rates of such sources for DECIGO and B-DECIGO. The result is that yearly detection of resolvable DCOs inspirals for the DECIGO is of order of $\mathcal{O}(10^2)$ for NS-NS, $\mathcal{O}(10^3)$ for BH-NS and $\mathcal{O}(10^5)$ for BH-BH systems, while for a much smaller scale B-DECIGO they are about $\mathcal{O}(10)$ for NS-NS, $\mathcal{O}(10^2)$ for BH-NS and $\mathcal{O}(10^5)$ for BH-BH systems. Taking into account that considerable part of these events would be detectable by ground-based GW observatories the significance of DECIGO/B-DECIGO could be substantial. Due to contamination by unresolved sources, both DECIGO and B-DECIGO will not be able to register lensed NS-NS or BH-NS systems, but the lensed BH-BH systems could be observed at the rate of about 50 per year in DECIGO. Smaller scale B-DECIGO will be able to detect a few lensed BH-BH systems per year. We also address the question of the magnification bias in the GW event catalogs of DECIGO and B-DECIGO.

Keywords: gravitational lensing, gravitational waves: sources

1. INTRODUCTION

First laboratory detections of gravitational waves (GWs) on Earth (Abbott et al. 2016) opened up a new branch of science – GW astronomy. Continuing efforts of LIGO/Virgo team (with now completed O1, O2 and O3 scientific runs) brought numerous detections of binary black hole (BH-BH) mergers (Abbott et al. 2019a), probably the first mixed black hole - neutron star (BH-NS) merger (Abbott et al. 2020a) and the first detection of binary neutron star (NS-NS) coalescence (Abbott et al. 2017a). The NS-NS merger was accompanied by identification of its electromagnetic (EM) counterpart and its afterglow was followed up at different EM wavelengths (Goldstein et al. 2017; Coulter et al. 2017). This observation moved multimessenger astronomy to the next level. Besides the tests of general relativity and modified gravity theories (Abbott et al. 2019b), strong bounds on the speed of GWs (Abbott et al. 2017b), GW astronomy has proven that (almost) all classes of double compact objects (DCOs): NS-NS, BH-NS, BH-BH really exist in

Nature. The event GW190425 is marginally compatible with NS-NS merger, so the existence of BH-NS systems still needs to be empirically proven. It is likely that this will happen soon.

Successful operation of ground-based interferometric detectors revived the interest in broadening the GW spectrum to lower frequencies (lower than 1 Hz) fundamentally inaccessible from the ground due to irremovable seismic noise. In particular, LISA was proposed (Amaro-Seoane et al. 2017) as a new generation space mission with a robust strain sensitivity level at frequencies between 0.1 mHz and 100 mHz over a science lifetime of at least 4 years. The technology behind LISA, an ESA-led mission expected to be launched by 2034, has been recently tested by the LISA Pathfinder experiment with outstanding results (Armano et al. 2016). The remaining decihertz band is the target of the DECihertz Interferometer Gravitational wave Observatory (DECIGO), a planned Japanese space-borne GW detector (Kawamura et al. 2019). Original DECIGO (Seto et al. 2001) or currently proposed smaller-scale version B-DECIGO (Sato et al. 2017) are aimed to cover the low-frequency band extending from the mHz to 100 Hz range. DECIGO would be able to detect inspiraling DCO — main targets to LIGO/Virgo, KAGRA or next generation ET, long time (weeks to years) before they enter the hectohertz band accessible from the ground. Moreover, the overlap with ground based GW detectors sensitivity bands is very advantageous since the joint detection with DECIGO and ground based detectors (e.g. ET) would greatly improve the parameter estimation of the binaries.

¹ Department of Astronomy, Beijing Normal University, Beijing 100875, China; zhuzh@bnu.edu.cn; caoshuo@bnu.edu.cn

² Institute of Physics, University of Silesia, 75 Pułku Piechoty 1, 41-500 Chorzów, Poland

³ School of Physics and Technology, Wuhan University, Wuhan 430072, China

⁴ National Centre for Nuclear Research, Pasteura 7, 02-093 Warsaw, Poland; Marek.Biesiada@ncbj.gov.pl

⁵ Department of Physics and Astronomy, University of California, Los Angeles, CA 90095-1547, USA

⁶ Department of Physics, Nagoya University, Nagoya, Aichi 464-8602, Japan

Reach of the DECIGO will be considerably higher than the next generation of ground based interferometric detectors, like the ET. With much higher volume probed, one may expect that non-negligible number of GW signals from coalescing DCOs would be gravitationally lensed. Gravitational lensing statistics and magnification cross-sections by galaxies has been discussed e.g. in (Zhu & Wu 1997; Zhu 1998). Rates of GW lensing for LIGO/Virgo have been calculated in Ng et al. (2018) and for the ET in Piórkowska et al. (2013); Biesiada et al. (2014); Ding et al. (2015); Li et al. (2018); Oguri (2019); Yang et al. (2019), respectively. The robust prediction is that the third generation of GW interferometric detectors would yield 50 - 100 lensed GW events per year. Strongly lensed GW signals, observed together with their electromagnetic (EM) counterparts, have been demonstrated to enhance our understanding regarding fundamental physics (Fan et al. 2017; Collett & Bacon 2017; Cao et al. 2019), dark matter (Liao et al. 2018), and cosmology (Serenio et al. 2010, 2011; Taylor & Gair 2012; Liao et al. 2017; Wei & Wu 2017). Gravitational lensing of GWs has been widely discussed concerning diffraction effects in lensed GW events (Liao et al. 2019; Takahashi & Nakamura 2003; Nakamura 1998), the waveform distortion caused by the gravitational lensing (Cao et al. 2014), the influence on the statistical signatures of black hole mergers (Dai et al. 2017).

In this paper we make predictions concerning detection rates of inspiraling DCO systems, confusion noise regarding unresolved DCO systems and finally gravitational lensing of GW signals detectable by the DECIGO.

2. GW BACKGROUND NOISE FROM DCO SYSTEMS

We start with the assessment of the background noise created by unresolved DCO systems. In next sections we will discuss the detection rate of such inspiraling systems and their lensing rate by background galaxies. In all these considerations one needs the detector's sensitivity curve and intrinsic DCO merger rates as input. We will discuss these issues below.

2.1. DECIGO sensitivity

DECIGO will be composed of four units of detectors. Each unit is planned to contain three drag-free spacecrafts to form a nearly regular triangle. These four units will be tilted 60° inwards relative to the ecliptic plane to keep its arm lengths nearly constant, and move around the sun with the orbital period of 1 yr. Centers of the triangular configuration of the units will form an equilateral triangle. The fourth one will be anchored to one of the units rotated 180° to form a Star of David configuration. Details concerning the DECIGO design could be found in Yagi & Seto (2011)

For the reference design parameters of DECIGO, one can prove (Yagi & Seto 2011) that a single triangular detector unit is equivalent to two L-shaped interferometers rotated by 45° . Their noises are uncorrelated and the noise spectrum of such an effective L-shaped DECIGO is

given by:

$$S_h(f) = 10^{-48} \times \left[7.05 \left(1 + \frac{f^2}{f_p^2} \right) + 4.80 \times 10^{-3} \times \frac{f^{-4}}{1 + \left(\frac{f}{f_p} \right)^2} + 5.33 \times 10^{-4} f^{-4} \right] Hz^{-1} \quad (1)$$

where $f_p = 7.36 Hz$.

The original DECIGO mission concept was proposed in 2001 by Seto et al. (2001). What now seems more realistic to be commissioned in the near future is a scaled smaller project called B-DECIGO. It will consist of three satellites in a 100 km equilateral triangle, having sun-synchronous dusk-dawn circular orbits 2000 km above the Earth Sato et al. (2017); Nakamura et al. (2016). With B-DECIGO operating, we will soon probe the decihertz window for the first time, completing the full gravitational spectrum. Therefore we extend our predictions to the B-DECIGO. We use the noise power spectrum density $S_h(f)$ for B-DECIGO proposed by Nakamura et al. (2016); Isoyama et al. (2018):

$$S_h(f) = 10^{-46} \times [4.040 + 6.399 \times 10^{-2} f^{-4} + 6.399 \times 10^{-3} f^2] Hz^{-1} \quad (2)$$

2.2. DCO merger rate from the population synthesis

Previous predictions concerning DECIGO (Yagi & Seto 2011; Yagi 2013) used an analytical approximation of the NS-NS merger rate as a function of redshift up to redshift $z = 5$. Moreover, they did not assess the BH-BH or BH-NS rates precisely. In this paper, we use the values of the intrinsic inspiral rates $\dot{n}_0(z_s)$ forecasted by Dominik et al. (2013) for each type of DCO at redshift slices spanning the range of $z \in [0.04; 17]$. These data, available at <https://www.syntheticuniverse.org> have been used in our previous papers (Biesiada et al. 2014; Ding et al. 2015), where one can find more details about them. For the current purpose it will be sufficient to recall the following facts. To account for the varied chemical composition of the Universe, they performed the cosmological calculations for two scenarios of galactic metallicity evolution, called “low-end” and “high-end”, respectively. Essentially, they modeled metallicity (in fact oxygen abundance, assumed to be correlated with metallicity) by empirical function of galaxy mass (derived from Schechter type distribution). The normalization factor of this relation is redshift dependent, which can be heuristically modeled by a relation, whose coefficient choice (in fact, it's a bit more complicated - see Dominik et al. (2013)) lead to two distinct metallicity evolution profiles. The first one called “high-end” predicts a median value of metallicity of $1.5 Z_\odot$ at $z \sim 0$. Another one, called “low-end” yields a median metallicity value of $0.8 Z_\odot$. Concerning binary system evolution from the ZAMS to the final formation of DCO binary system (NS-NS, NS-BH or BH-BH) we will consider four scenarios: standard, optimistic common envelope, delayed SN explosion and high BH natal kicks as specified in Dominik et al. (2013), where the reader is referred to for more details. In previous papers cited above, the median masses: $1.2M_\odot$ for NS-NS, $3.2M_\odot$ for BH-NS, and $6.7M_\odot$ for BH-BH

were used according to [Dominik et al. \(2012\)](#). However, these were values obtained under the assumption of solar metallicity of initial binary systems. Such scenario was a right guess before the first detections of GWs. Now, the data collected with the LIGO/Virgo detectors demonstrated that observed chirp masses (in particular of BH-BH systems) are much higher. Hence one is forced to change the aforementioned assumption. Moreover, as we will see further on, probability density of DCO inspirals (observable by DECIGO) peak at $z=2$, when the metallicity was significantly sub-solar. Therefore, guided by the real data gathered so far we will adopt different values – according to [Abbott et al. \(2019a\)](#). We will assume the median value of BH-BH systems chirp masses reported in their Table III. Since the data on BH-NS systems is more scarce, we will take the value of [Abbott et al. \(2020b\)](#). Hence, the following chirp masses will be adopted by us as representative of DCO inspiraling systems: $1.2 M_\odot$ for NS-NS, $6.09 M_\odot$ for BH-NS, and $24.5 M_\odot$ for BH-BH. In order to comply with the assumptions underlying population synthesis simulation, we assume flat Λ CDM cosmology with $H_0 = 70 \text{ km s}^{-1} \text{ Mpc}^{-1}$ and $\Omega_m = 0.3$.

2.3. GW background from unresolved DCO systems

Magnitude of a stochastic GW background is usually characterized by its fractional energy density per logarithmic frequency interval:

$$\Omega_{GW} = \frac{1}{\rho_{cr}} \frac{d\rho_{GW}}{d \ln f} \quad (3)$$

where $\rho_{cr} = 3H_0^2/8\pi G$ is the critical energy density of the Universe. Let us note, that in the context of a confusion noise due to unresolved sources, the distinction between background and foreground is not clear-cut. We will call it background.

According to [Phinney \(2001\)](#) one can conveniently calculate the energy density parameter Ω_{GW}^{DCO} corresponding to the unresolved signals from the DCO systems, as

$$\Omega_{GW}^{DCO} = \frac{8\pi^{5/3}}{9c^2 H_0^2} (GM)^{5/3} f^{2/3} \int_0^\infty \frac{\dot{n}(z)}{(1+z)^{4/3} H(z)} dz \quad (4)$$

where M is the chirp mass of the DCO system (i.e. NS-NS, BH-NS or BH-BH binary), $\dot{n}(z)$ is the DCO merger rate per proper time per comoving volume at redshift z , and the Hubble parameter $H(z)$ is given by $H(z)^2 = H_0^2[\Omega_m(1+z)^3 + 1 - \Omega_m]$. Calculating numerically the integral in Eq.(4) one obtains:

$$\Omega_{GW}^{DCO} = \Omega_0^{DCO} \left(\frac{H_0}{70 \text{ km s}^{-1} \text{ Mpc}^{-1}} \right)^{-3} \times \left(\frac{M}{M_{DCO}} \right)^{5/3} \left(\frac{f}{1 \text{ Hz}} \right)^{2/3} \quad (5)$$

where M_{DCO} is the median value of the DCO considered, i.e. $(M_{NSNS}; M_{BHNS}; M_{BHBH}) = (1.22; 6.09; 24.5) M_\odot$ and values of Ω_0^{DCO} coefficients are reported in Table 1.

In order to compare with the detector's noise power spectrum the normalized energy density Ω_{GW}^{DCO} should be expressed as the total sky-averaged GW spectrum:

$$S_h^{GW,DCO} = \frac{4}{\pi} f^{-3} \rho_{cr} \Omega_{GW}^{DCO}. \quad (6)$$

The background spectrum of three DCO populations imposed on the DECIGO sensitivity curve is shown in Figure 1. Let us note that B-DECIGO will be much less contaminated from the unresolved DCO systems, yet the events like those detected by LIGO/Virgo will be detectable enabling their discovery and study long before they will enter the ground-based detectors sensitivity band. As discussed in details in [Isoyama et al. \(2018\)](#), time to coalescence can be estimated as: $t_c = 1.03 \times 10^6 \text{ s} (M_z/30.1 M_\odot)^{-5/3} (f/0.1 \text{ Hz})^{-8/3}$, which means that GW150914 and GW170817 could have been visible in (B-)DECIGO band for ~ 10 days and ~ 7 yrs prior to coalescence with large numbers of GW cycles (10^5 and 10^7 , respectively).

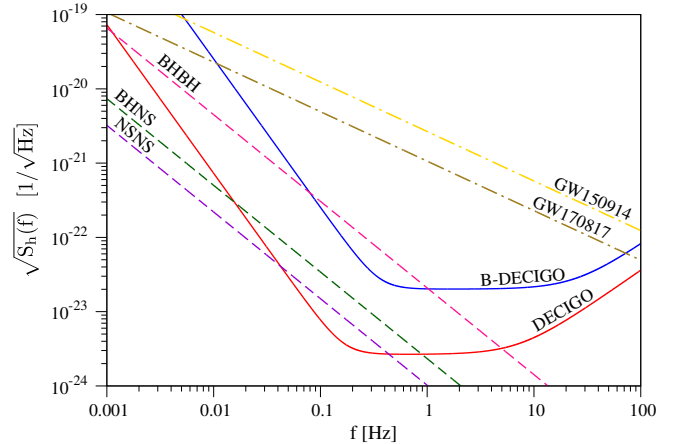


Figure 1. Confusion noise due to DCO systems (NS-NS, BH-NS and BH-BH) superimposed on the noise spectrum density for DECIGO and B-DECIGO. Inspiral rates correspond to the standard scenario and “low-end” metallicity evolution. The effective squared spectrum density corresponding to GW150914 and GW170817 events has been also included.

3. DETECTION RATE FOR UNLENSED EVENTS

Matched filtering signal-to-noise ratio for a single detector reads ([Taylor & Gair 2012](#)):

$$\rho = 8\Theta \frac{r_0}{d_L(z_s)} \left(\frac{M_z}{1.2 M_\odot} \right)^{5/6} \sqrt{\zeta(f_{max})} \quad (7)$$

where d_L is the luminosity distance to the source, Θ is the orientation factor capturing part of sensitivity pattern due to (usually non-optimal) random relative orientation of DCO system with respect to the detector (more details below). Zeta parameter capturing the overlap between the signal and the detector's sensitivity band width is defined as:

$$\zeta(f_{max}) = \frac{1}{x_{7/3}} \int_0^{2f_{max}} \frac{df (\pi M_\odot)^2}{(\pi f M_\odot)^{7/3} S_h(f)}$$

where $2f_{max}$ is the wave frequency at which the inspiral detection template ends and $x_{7/3} = (\pi M_\odot)^{-1/3} f_{7/3}$ (see below for definition of $f_{7/3}$). Calculating ζ factor with the above definition one obtains $\zeta(f_{max}) \approx 1$ for all DCO systems considered. However, the confusion noise of unresolved systems will influence our ability to detect inspiraling DCO systems. Therefore, we should use the

modified noise spectrum $S_h(f) + S_h^{GW,DCO}(f)$ (system by system, and scenario by scenario). There are two ways to do that, both leading to the same results. First, is the take the detector's characteristic distance r_0 (defined below) and hence $x_{7/3}$ calculated from the detector's noise $S_h(f)$ but modified noise in the calculation of $\zeta(f_{max})$ (in $x_{7/3}$ noise is not modified). In this case ζ factors are considerably smaller. Second approach is to consider noise spectrum modified by DCO confusion noise and regard different detector's characteristic distances r_0 (system by system and scenario by scenario). Then $\zeta(f_{max}) \approx 1$ is valid. By r_0 we denote the detector's characteristic distance parameter, which can be estimated according to:

$$r_0^2 = \frac{5}{192\pi^{4/3}} \left(\frac{3}{20}\right)^{5/3} \frac{(GM_\odot)^{5/3}}{c^3} f_{7/3}$$

where:

$$f_{7/3} = \int_0^\infty \left[f^{7/3} S_h(f) \right]^{-1} df$$

Using DECIGO sensitivity Eq.(1) one gets:

$$r_0 = 6709 \text{ Mpc.}$$

Similarly, from the B-DECIGO sensitivity given by Eq.(2) one obtains $r_0 = 535 \text{ Mpc.}$, meaning that B-DECIGO will be able to probe about a 1000 times smaller volume than DECIGO.

The orientation factor Θ is defined as

$$\Theta = 2[F_+^2(1 + \cos^2 \iota)^2 + 4F_\times^2 \cos^2 \iota]^{1/2} \quad (8)$$

where $F_+ = \frac{1}{2}(1 + \cos^2 \theta) \cos 2\phi \cos 2\psi - \cos \theta \sin 2\phi \sin 2\psi$ and $F_\times = \frac{1}{2}(1 + \cos^2 \theta) \cos 2\phi \sin 2\psi + \cos \theta \sin 2\phi \cos 2\psi$ are the interferometer strain responses to different polarizations of gravitational wave. The angles (θ, ϕ) describe orientation (polar angles) of direction to the source with respect to the detector plane, (ψ, ι) are the angles describing DCO orbit orientation with respect to the plane tangent to the celestial sphere at source location (so called polarization angle and inclination). The above formulae for $F_{+/\times}$ are for just one L-shaped detector $F_{I;+/\times}$, for the second one it would be $F_{II;+/\times} = F_{I;+/\times}(\theta, \phi - \pi/4, \psi, \iota)$.

Probability distribution for Θ calculated under assumption of uncorrelated orientation angles $(\theta, \phi, \psi, \iota)$ is known to be of the following form (Finn 1996):

$$P_\Theta(\Theta) = 5\Theta(4 - \Theta)^3/256, \quad \text{if } 0 < \Theta < 4 \quad (9)$$

$$P_\Theta(\Theta) = 0, \quad \text{otherwise}$$

The yearly detection rate of DCO sources originating at redshift z_s and producing the signal with SNR exceeding the detector's threshold $\rho_0 = 8$ (assumption made in previous DECIGO studies (Yagi & Seto 2011; Isoyama et al. 2018)) can be expressed as:

$$\dot{N}(> \rho_0 | z_s) = \int_0^{z_s} \frac{d\dot{N}(> \rho_0)}{dz} dz \quad (10)$$

where

$$\frac{d\dot{N}(> \rho_0)}{dz_s} = 4\pi \left(\frac{c}{H_0}\right)^3 \frac{\dot{n}_0(z_s)}{1 + z_s} \frac{\tilde{r}^2(z_s)}{E(z_s)} C_\Theta(x(z_s, \rho_0)) \quad (11)$$

$\dot{n}_0(z_s)$ denotes intrinsic coalescence rate at redshift z_s , $C_\Theta(x) = \int_x^\infty P_\Theta(\Theta) d\Theta$ and $x(z, \rho) = \frac{\rho}{8} (1 + z)^{1/6} \frac{c}{H_0} \frac{\tilde{r}(z)}{r_0} \left(\frac{1.2 M_\odot}{\mathcal{M}_0}\right)^{5/6} \zeta(f_{max})^{-1/2}$, i.e. $x(z, \rho)$ is a transformed Eq. (7) where Θ is treated as a variable.

Throughout this paper we use the values of inspiral rates $\dot{n}_0(z_s)$ obtained with **StarTrack** evolutionary code. The results are summarized in Table 2. Probability density of DCO inspiral events as a function of redshift is shown in Fig 2. One can see that even though B-DECIGO is considerably smaller scale enterprize, it would be able to register tens of resolvable NS-NS inspirals and hundred thousands of resolvable BH-BH inspirals per year.

4. LENSED GW SIGNALS STATISTICS

We assume that the population of lenses comprise only elliptical galaxies modeled as singular isothermal spheres (SIS). This assumption is supported by galaxy strong lensing studies (Koopmans et al. 2009). Einstein radius, which is a characteristic angular scale of separation between images in the SIS model can be expressed as: $\theta_E = 4\pi \left(\frac{\sigma}{c}\right)^2 \frac{d_A(z_l, z_s)}{d_A(z_s)}$, where σ is the velocity dispersion of stars in lensing galaxy, $d_A(z_l, z_s)$ and $d_A(z_s)$ are angular diameter distances between the lens and the source and to the source, respectively (Cao et al. 2012a, 2015). Calculations are simplified if one expresses the angular distance of the image from the center of the lens θ and the angular position of the source β as dimensionless parameters: $x = \frac{\theta}{\theta_E}$, $y = \frac{\beta}{\theta_E}$. Then the necessary condition for strong lensing (appearance of multiple images) is $y < 1$. Brighter I_+ and fainter image I_- form at locations $x_\pm = 1 \pm y$ with magnifications: $\mu_\pm = \frac{1}{y} \pm 1$. Gravitationally lensed GW signal would come from these two images with appropriate relative time delay $\Delta t = \Delta t_0(\sigma, z_l, z_s)y$ (for details see (Piórkowska et al. 2013; Biesiada et al. 2014)) and with different amplitudes: $h_\pm = \sqrt{\mu_\pm} h(t) = \sqrt{\frac{1}{y} \pm 1} h(t)$ where $h(t)$ denotes the intrinsic amplitude (i.e. the one which would have been observed without lensing). In order to observe lensed image I_+ or I_- the detected SNR ρ_\pm must exceed the threshold for detection $\rho_0 = 8$. This happens, if the misalignment of the source with respect to the optical axis of the lens satisfies:

$$y_\pm \leq y_{\pm, max} = \left[\left(\frac{8}{\rho_{intr.}} \right)^2 \mp 1 \right]^{-1} \quad (12)$$

where $\rho_{intr.}$ is the intrinsic SNR of the (unlensed) source.

Consequently, the cross section for lensing is (see e.g.(Piórkowska et al. 2013)):

$$S_{cr, \pm}(\sigma, z_l, z_s, \rho) = 16\pi^3 \left(\frac{\sigma}{c}\right)^4 \left(\frac{\tilde{r}_{ls}}{\tilde{r}_s}\right)^2 y_{\pm, max}^2 \quad (13)$$

and the optical depth for lensing leading to magnifications of I_+ and I_- images above the threshold reads:

$$\tau_\pm(z_s, \rho) = \frac{1}{4\pi} \int_0^{z_s} dz_l \int_0^\infty d\sigma 4\pi \left(\frac{c}{H_0}\right)^3 \times \frac{\tilde{r}_l^2}{E(z_l)} S_{cr, \pm}(\sigma, z_l, z_s) \frac{dn}{d\sigma}. \quad (14)$$

Table 1

Numerical factors Ω_0^{DCO} in the Eq.(5) for different classes of DCO systems under different evolutionary scenarios, assuming “low-end” and “high-end” metallicity evolution.

$\Omega_0^{DCO} \times 10^{-12}$				
Evolutionary scenario	standard	optimistic	delayed SN	high BH kicks
NS-NS				
low-end metallicity	1.33	10.26	1.51	1.34
high-end metallicity	2.17	9.95	2.44	2.14
BH-NS				
low-end metallicity	6.94	18.79	3.74	0.68
high-end metallicity	4.10	14.30	2.22	0.48
BH-BH				
low-end metallicity	554.58	2983.01	427.78	20.88
high-end metallicity	368.68	2026.12	262.41	13.65

Table 2

Yearly detection rate of inspiraling DCOs of different classes under different evolutionary scenarios, assuming “low-end” and “high-end” metallicity evolution. Predictions for the DECIGO and B-DECIGO. Yearly detection rates of resolvable DCO systems are reported.

Yearly detection rate for DECIGO				
Evolutionary scenario	standard	optimistic CE	delayed SN	high BH kicks
NS-NS				
low-end metallicity	233.1	119.	335.5	3054.4
high-end metallicity	439.6	203.9	707.3	8807.7
BH-NS				
low-end metallicity	2688.9	1239.5	1838.6	1877.6
high-end metallicity	2000.	1314.6	1614.5	1613.7
BH-BH				
low-end metallicity	207755.2	384698.	178991.7	20125.8
high-end metallicity	166436.	360001.5	145583.5	15379.5
TOTAL				
low-end metallicity	210677.2	386056.5	181165.8	25057.8
high-end metallicity	168875.6	361520	147905.3	25800.9

Yearly detection rate for B-DECIGO				
Evolutionary scenario	standard	optimistic CE	delayed SN	high BH kicks
NS-NS				
low-end metallicity	27.9	19.5	38.1	109.7
high-end metallicity	54.4	42.2	78.7	139.
BH-NS				
low-end metallicity	172.6	175.9	138.7	91.1
high-end metallicity	182.8	267.8	142.4	90.7
BH-BH				
low-end metallicity	54049.4	94584.8	47625.3	7015.
high-end metallicity	53220.2	112221.1	49773.8	5078.8
TOTAL				
low-end metallicity	54249.9	94780.2	47802.1	7215.8
high-end metallicity	53457.4	112531.1	49994.9	5308.5

We model the velocity dispersion distribution in the population of lensing galaxies as a modified Schechter function $\frac{dn}{d\sigma} = n_* \left(\frac{\sigma}{\sigma_*}\right)^\alpha \exp\left(-\left(\frac{\sigma}{\sigma_*}\right)^\beta\right) \frac{\beta}{\Gamma(\frac{\alpha}{\beta})} \frac{1}{\sigma}$ with parameters n_*, σ_*, α and β taken after Choi, Park & Vogeley (2007). The choice of this particular model, despite the existence of more recent data on velocity dispersion distribution functions is motivated by its best representing the pure elliptical galaxy population in agreement with our model assumption (Biesiada et al. 2014; Cao et al.

2012b).

Under the above assumptions, total optical depth for lensing is:

$$\tau_{\pm} = \frac{16}{30} \pi^3 \left(\frac{c}{H_0}\right)^3 \tilde{r}_s^3 \left(\frac{\sigma_*}{c}\right)^4 n_* \frac{\Gamma\left(\frac{4+\alpha}{\beta}\right)}{\Gamma\left(\frac{\alpha}{\beta}\right)} y_{\pm, max}^2. \quad (15)$$

The above formula is valid only in the case of a continuous search. If instead the survey has a finite duration T_{surv} some of the events, i.e. those whose signals come

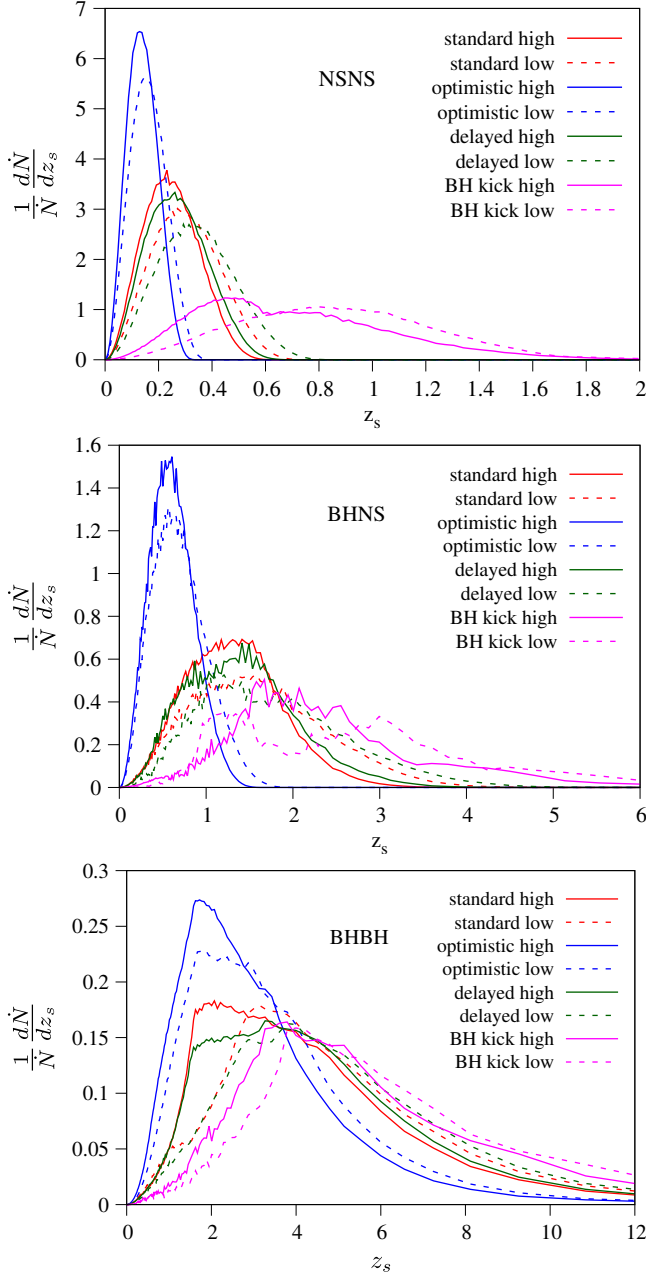


Figure 2. Probability density of DCO inspiral events as a function of redshift for the DECIGO. Different colors refer to different scenarios: red – standard, blue – OCE, green – delayed SN, magenta – high BH kicks. Solid line corresponds to the high-end metallicity evolution, dashed line – low-end metallicity.

near the beginning or the end of the survey, would be lost because of lensing time delay. In other words we would register the signal from just one image and cannot tell that in fact the event was lensed. Finite duty cycle of the detector influences the optical depth τ_{\pm} . Namely, it should be corrected as:

$$\tau_{\Delta t, \pm} = \tau \left[1 - \frac{1}{7} \frac{\Gamma\left(\frac{\alpha+8}{\beta}\right)}{\Gamma\left(\frac{\alpha+4}{\beta}\right)} \frac{\Delta t_{*, \pm}}{T_{surv}} \right] \quad (16)$$

where $\Delta t_{*, \pm} = \frac{32\pi^2}{H_0} \tilde{r}_s \left(\frac{\sigma_*}{c}\right)^4 y_{\pm, max}$ (for detailed calculations see Piórkowska et al. (2013)). This correction

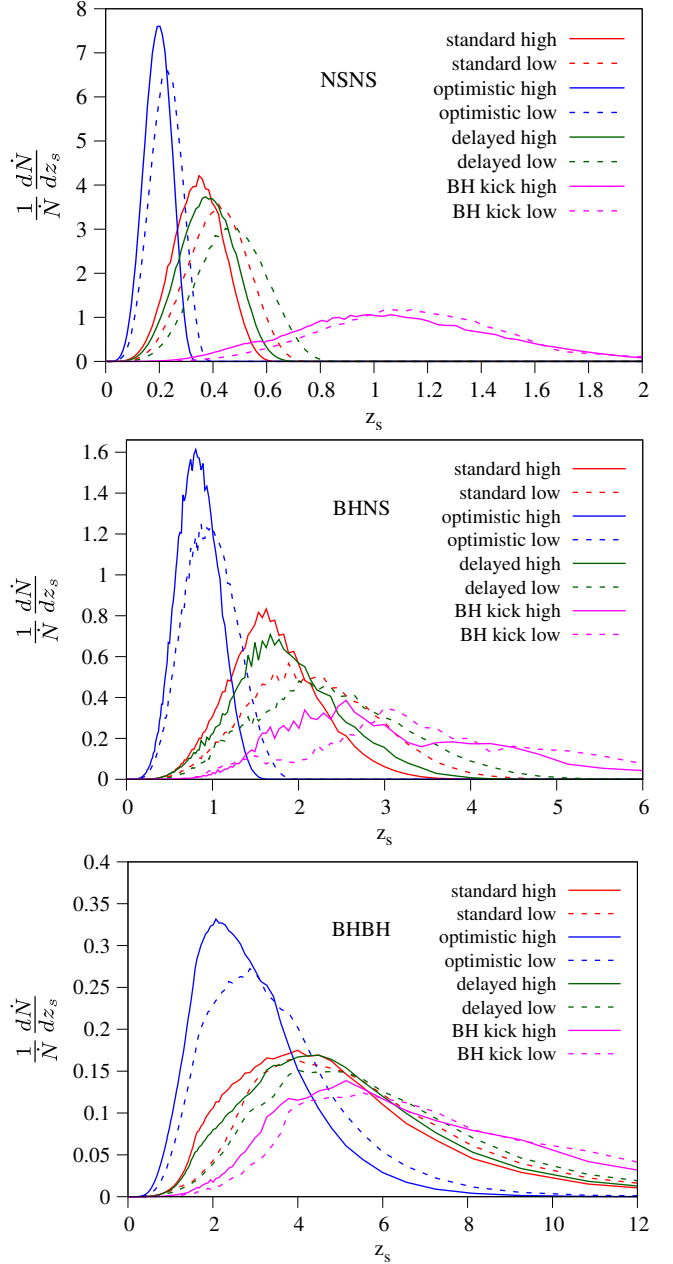


Figure 3. Differential lensing rate $\frac{1}{N_{lensed}} \frac{dN_{lensed}}{dz}$ (as a function of source redshift) of DCO inspiraling binaries for different evolutionary scenarios (solid lines and dashed lines corresponds respectively to high-end and low-end metallicity evolution). Predictions for the DECIGO 4 years operation.

is particularly important here, because the DECIGO and B-DECIGO missions are planned for $T_{surv} = 4$ yr. We present predictions for the first year of operation and for the total 4 yrs of nominal duration. Moreover, we conservatively assume that the lensed system is intrinsically loud enough to exceed the detector's threshold $\rho_0 = 8$ and we assume that the fainter image exceeds the threshold. This means that we only consider $y_{max} = y_{-, max} = 0.5$, according to Eq. (12).

Cumulative yearly detection of lensed events up to the

source redshift z_s can be calculated as:

$$\dot{N}_{lensed}(z_s) = \int_0^{z_s} \tau_{\Delta t}(z_s, y_{max}, T_{surv}) \frac{d\dot{N}(> \rho_0)}{dz} dz. \quad (17)$$

The results for both DECIGO and B-DECIGO are shown in Table 3. In Fig. 3 normalized differential lensing rate (as a function of redshift) is displayed. One can verify that DECIGO in its original design would be able to register 5 – 6 strongly lensed NS-NS (or BH-NS) systems, if the contamination from unresolved sources is neglected. These systems could be accompanied by the EM counterpart during their final merger phase detectable by ground based interferometric detectors. Hence, they are the most promising lensed sources enabling e.g precise cosmological inference (Liao et al. 2017) or probing dark matter substructure in lensing galaxies (Liao et al. 2018). However, contamination by unresolved systems (predominantly BH-BH systems) make the chances of detecting lensed NS-NS or BH-NS binaries negligible. On the other hand tens of lensed inspirals could be seen from the BH-BH binary systems both in DECIGO and B-DECIGO.

5. CONCLUSIONS

In this paper we have made the predictions of yearly detection rates of GW signals from the DCO inspirals detectable in the future decihertz space-borne detectors DECIGO and its smaller scale version B-DECIGO. All previous papers concerning DECIGO used only analytical estimates of NS-NS merger rates up to $z = 5$. In our calculations, we have used for the first time the *StarTrack* population synthesis results concerning intrinsic merger rates at different redshifts of distinct classes of DCO systems: NS-NS, BH-NS and BH-BH binaries. Now, when more accurate estimates of merger rates from the LIGO/Virgo data are available (Abbott et al. 2019a) one can make a comparison between *StarTrack* predictions and real data estimates (Hou et al. 2020b). It turns out that “low-end” metallicity predictions are in agreement with those based on LIGO/Virgo derived merger rates.

We have also estimated the stochastic noise levels due to unresolved DCO systems. The conclusion is that DECIGO would be significantly contaminated by unresolved BH-BH binary systems, while the level of this stochastic noise component is not so relevant for B-DECIGO. Concerning the DCO yearly detection rate its order of magnitude ranges from 10^2 for NS-NS, 10^3 for BH-NS systems to 10^6 for BH-BH systems in DECIGO. Respective rates for the B-DECIGO are 10 (NS-NS), 10^2 (BH-NS) and 10^5 (BH-BH).

The detector’s distance parameter r_0 for the DECIGO is about 4 times bigger than for the ET, meaning that DECIGO will probe 64 times bigger volume than the next generation of ground based detectors. Hence, we addressed the issue of gravitationally lensed DCO inspirals observable by the DECIGO. For the completeness of discussion we considered B-DECIGO as well, even though B-DECIGO’s r_0 is about 3 times smaller than for the ET. Our basic assessment was performed under assumption that the GW source is intrinsically loud (i.e. would be detectable without lensing). The result is that due to contamination of unresolved systems, either DECIGO or B-DECIGO will not be able to register any lensed

NS-NS or BH-NS inspirals. However, they could register up to $O(10)$ lensed BH-BH inspirals.

In the appendix we enrich our discussion relaxing the $\rho_{intr.} \geq 8$ assumption and consider intrinsically faint signals, i.e. those being detectable exclusively due to lensing magnification. Such inclusion of lensing magnification could significantly enlarge the statistics of lensed events with intrinsic SNR $\rho_{intr.} \geq 8$ for both DECIGO and B-DECIGO. The appendix also addresses the question of the magnification bias in the full inspiral GW event catalogs of DECIGO and B-DECIGO. One finds out that the magnification bias is of the order of $10^{-3} - 10^{-4}$, which means that the cosmological inferences drawn from these catalogs would not be affected very much.

Let us stress that DECIGO and B-DECIGO would be able to register inspiral signals from the DCOs weeks or years (the higher redshifted chirp mass the shorter time of passing through DECIGO band) before they enter the high frequency band of ground-based detectors to finally end their lives in energetic mergers. Having in mind this circumstance and the benefits that are expected from registering lensed GW one would expect that DECIGO’s detections of lensed GW signals could trigger a concerted efforts for searching strong lenses in the EM domain at possible locations suggested by the DECIGO. This would be very profitable in many aspects, in particular for identifying the host galaxy before the merger and despite of no bright EM counterpart as it was the case to the BH-BH mergers registered so far. In the light of considerable rate of DCO inspiral signals detectable by the DECIGO, one should be concerned how to distinguish gravitationally lensed signals. This issue deserves separate studies on simulated mock catalogs of signals. It is usually expected that lensed signals would have the same temporal behaviour (frequency and its rate of change) differing only by amplitude due to magnification and come to the detector after some delay (Dai et al. 2017; Ng et al. 2018; Biesiada et al. 2014). This is a very reasonable expectation for lensed signals from the final merger phase. However, unlike the ground-based detector where one registers a transient event, DECIGO would observe lensed events in an adiabatic inspiral phase as two (or more) unresolved images, likely producing interference patterns in the waveforms (Hou et al. 2020a). Let us note that interference beat patterns are interesting on their own. This topic is besides the scope of the present paper which focused only on the statistics of GW lensing and is the subject of a separate study Hou et al. (2020b).

ACKNOWLEDGMENTS

We would like to thank the referee for constructive comments which allowed to improve the original version substantially. This work was supported by National Key R&D Program of China No. 2017YFA0402600; the National Natural Science Foundation of China under Grants Nos. 11690023, 11373014, and 11633001; Beijing Talents Fund of Organization Department of Beijing Municipal Committee of the CPC; the Strategic Priority Research Program of the Chinese Academy of Sciences, Grant No. XDB23000000; the Interdiscipline Research Funds of Beijing Normal University; and the Opening Project of Key Laboratory of Computational Astrophysics, National Astronomical Observatories, Chinese Academy of

Sciences. This work was initiated at Aspen Center for Physics, which is supported by National Science Foundation grant PHY-1607611. This work was partially supported by a grant from the Simons Foundation. M.B. is grateful for this support. S.H. was supported by Project funded by China Postdoctoral Science Foundation (No. 2020M672400).

APPENDIX - LENSING OF INTRINSICALLY FAINT GW SOURCES

Gravitational lensing magnifies the lensed images of the source. Therefore, one can relax the assumption that sources should be intrinsically loud enough to be detected without lensing and treat their signal to noise parameter ρ as a free one. In such a case one would get estimates for the population of DCO systems detectable exclusively due to gravitational lensing. In other words this would provide forecasts for magnification bias in the catalog of lensed DCO inspirals. We will follow the strategy used in Ding et al. (2015) in the case of the ET. Therefore, instead of Eq. (11) we have to start with the differential inspiral rate per redshift and per SNR parameter ρ :

$$\frac{\partial^2 \dot{N}}{\partial z_s \partial \rho} = 4\pi \left(\frac{c}{H_0} \right)^3 \frac{\dot{n}_0(z_s) \tilde{r}^2(z_s) P_\Theta(x(z_s, \rho))}{1 + z_s E(z_s)} \frac{x(z_s, \rho)}{\rho} \quad (18)$$

then one should calculate cross-sections $S_{cr, \pm}$ and optical depths τ_{\pm} for lensing separately for each image I_+ or I_- .

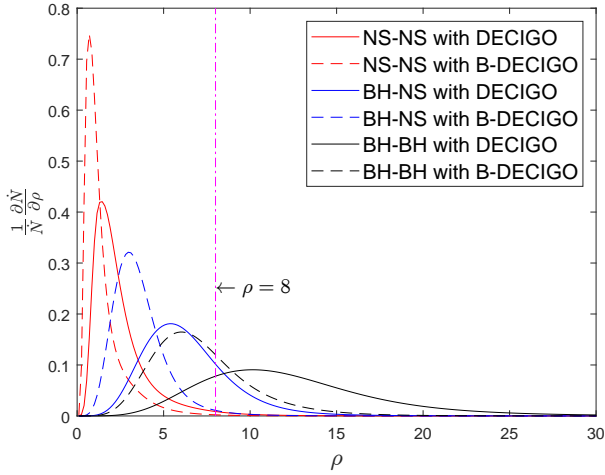


Figure 4. The normalized differential yearly detection rates $\frac{1}{N} \frac{\partial \dot{N}}{\partial \rho}$ v.s. the intrinsic SNR ρ . “Low-end” metallicity galaxy evolution and the standard model of DCO formation are assumed.

The final result will be the lensing rate of intrinsically faint ($\rho < \rho_0$) DCOs having I_+ or I_- images magnified above the threshold ρ_0 :

$$\dot{N}_{lensed, \pm} = \int_0^{z_{max}} dz_s \int_0^{\rho_0} \tau_{\Delta t, \pm}(z_s, \rho) \frac{\partial^2 \dot{N}}{\partial z_s \partial \rho} d\rho \quad (19)$$

or differential lensing rates with respect to ρ or z_s respectively:

$$\frac{d\dot{N}_{lensed, \pm}}{d\rho} = \int_0^{z_{max}} \tau_{\Delta t, \pm}(z_s, \rho) \frac{\partial^2 \dot{N}}{\partial z_s \partial \rho} dz_s \quad (20)$$

$$\frac{d\dot{N}_{lensed, \pm}}{dz_s} = \int_0^{\rho_0} \tau_{\Delta t, \pm}(z_s, \rho) \frac{\partial^2 \dot{N}}{\partial z_s \partial \rho} d\rho. \quad (21)$$

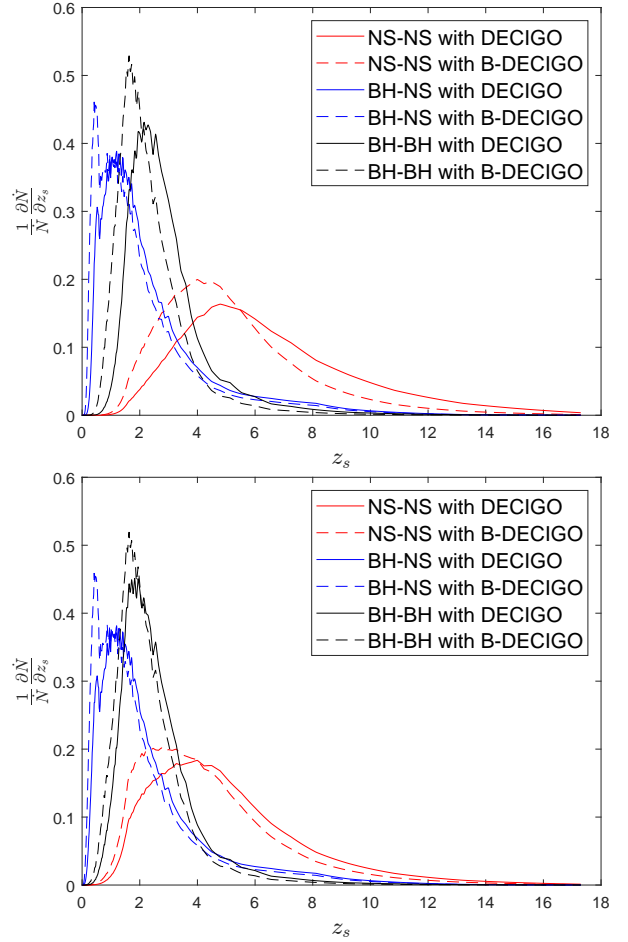


Figure 5. The normalized differential yearly detection rates $\frac{1}{N} \frac{\partial \dot{N}}{\partial z_s}$ v.s. the source redshift z_s . Upper figure corresponds to $\rho_{intr} < 8$ for the I_- image. The lower one corresponds to the I_- image including both $\rho_{intr} < 8$ and $\rho_{intr} \geq 8$. Low-end metallicity galaxy evolution and standard model of DCO formation are assumed.

Table 4 contains the results of predicted intrinsically faint lensed GW events for which the the I_- image is magnified above threshold $\rho_0 = 8$ for DECIGO and B-DECIGO. As one can see, inclusion of lensing magnification of intrinsically faint events would significantly enlarge the statistics of lensed events with intrinsic SNR $\rho_{intr} \geq 8$ (see Tab. 3). This conclusion is true both for DECIGO and B-DECIGO.

The normalized differential yearly detection rates $\frac{1}{N} \frac{\partial \dot{N}}{\partial \rho}$ of lensed events as functions of the intrinsic SNR ρ for various types of DCOs to be observed by DECIGO and B-DECIGO are displayed in Fig. 4.

Figure 5 shows the normalized differential yearly detection rates $\frac{1}{N} \frac{\partial \dot{N}}{\partial z_s}$ of lensed events as functions of the source redshift z_s . The top panel illustrates lensed faint systems with $\rho_{intr} < 8$ with the I_- image magnified above the threshold. In other words, both images will be registered by DECIGO or B-DECIGO. In the lower panel differential detection rate is shown for systems of both $\rho_{intr} < 8$ and $\rho_{intr} \geq 8$, i.e. for the total catalog of lensed GW events of DECIGO or B-DECIGO. For the sake of transparency only standard scenario of DCO formation with “low-end” metallicity evolution is

Table 3

Expected numbers of lensed GW events from inspiraling DCOs of different classes under different evolutionary scenarios, assuming “low-end” and “high-end” metallicity evolution. Predictions for the DECIGO and B-DECIGO under assumption of $T_{surv} = 4 \text{ yrs}$.

DECIGO				
Evolutionary scenario	standard	optimistic CE	delayed SN	high BH kicks
NS-NS				
low-end metallicity	0.	0.	0.	0.07
high-end metallicity	0.	0.	0.	0.29
BH-NS				
low-end metallicity	0.2	0.02	0.15	0.38
high-end metallicity	0.21	0.03	0.2	0.39
BH-BH				
low-end metallicity	66.91	58.12	62.86	10.04
high-end metallicity	65.07	71.28	61.41	8.46
B-DECIGO				
Evolutionary scenario	standard	optimistic CE	delayed SN	high BH kicks
NS-NS				
low-end metallicity	0.	0.	0.	0.
high-end metallicity	0.	0.	0.	0.
BH-NS				
low-end metallicity	0.2	0.02	0.15	0.38
high-end metallicity	0.21	0.03	0.2	0.39
BH-BH				
low-end metallicity	9.25	5.42	9.2	2.73
high-end metallicity	13.66	10.94	14.78	2.25

Table 4

Expected numbers of lensed GW events observed by DECIGO and B-DECIGO with $\rho_{intr} < 8$ for which the L_{-} image is magnified above threshold $\rho_0 = 8$. We assumed the survey duration $T_{surv} = 4 \text{ yrs}$. Nomenclature of DCO formation scenarios and galaxy metallicity evolution follows that of [Dominik et al. \(2013\)](#).

DECIGO				
Evolutionary scenario	standard	optimistic CE	delayed SN	high BH kicks
NS-NS				
low-end metallicity	0.02	0.03	0.03	0.64
high-end metallicity	0.06	0.05	0.10	0.98
BH-NS				
low-end metallicity	0.83	0.38	0.49	0.13
high-end metallicity	0.86	0.48	0.52	0.12
BH-BH				
low-end metallicity	26.6	66.1	21.5	0.62
high-end metallicity	21.1	66.1	16.3	0.45
TOTAL				
low-end metallicity	27.5	66.5	22.0	1.39
high-end metallicity	22.0	66.6	16.9	1.55
B-DECIGO				
Evolutionary scenario	standard	optimistic CE	delayed SN	high BH kicks
NS-NS				
low-end metallicity	0.002	0.003	0.002	0.01
high-end metallicity	0.004	0.004	0.005	0.02
BH-NS				
low-end metallicity	0.122	0.054	0.08	0.06
high-end metallicity	0.112	0.064	0.08	0.04
BH-BH				
low-end metallicity	24.3	31.5	22.0	2.39
high-end metallicity	22.4	34.	20.1	1.98
TOTAL				
low-end metallicity	24.4	31.6	22.1	2.5
high-end metallicity	22.5	34.6	20.2	2.0

Table 5

Expected numbers of lensed GW events observed by DECIGO and B-DECIGO with $\rho_{intr} < 8$ for which the I_+ image is magnified above threshold $\rho_0 = 8$. Other assumptions and terminology – like in Table 4.

DECIGO				
Evolutionary scenario	standard	optimistic CE	delayed SN	high BH kicks
NS-NS				
low-end metallicity	0.04	0.04	0.067	2.31
high-end metallicity	0.14	0.061	0.254	4.08
BH-NS				
low-end metallicity	3.94	1.30	2.43	0.68
high-end metallicity	4.16	1.72	2.60	0.630
BH-BH				
low-end metallicity	135.6	335.7	109.4	3.11
high-end metallicity	107.4	333.0	82.6	2.29
TOTAL				
low-end metallicity	139.6	348.7	111.9	6.1
high-end metallicity	111.7	334.8	85.4	7.0
B-DECIGO				
Evolutionary scenario	standard	optimistic CE	delayed SN	high BH kicks
NS-NS				
low-end metallicity	0.002	0.003	0.003	0.017
high-end metallicity	0.005	0.005	0.008	0.032
BH-NS				
low-end metallicity	0.33	0.11	0.22	0.23
high-end metallicity	0.29	0.13	0.22	0.17
BH-BH				
low-end metallicity	120.0	141.0	109.4	12.1
high-end metallicity	111.4	158.1	100.7	10.0
TOTAL				
low-end metallicity	120.3	141.1	109.6	12.3
high-end metallicity	111.7	158.2	100.9	10.2

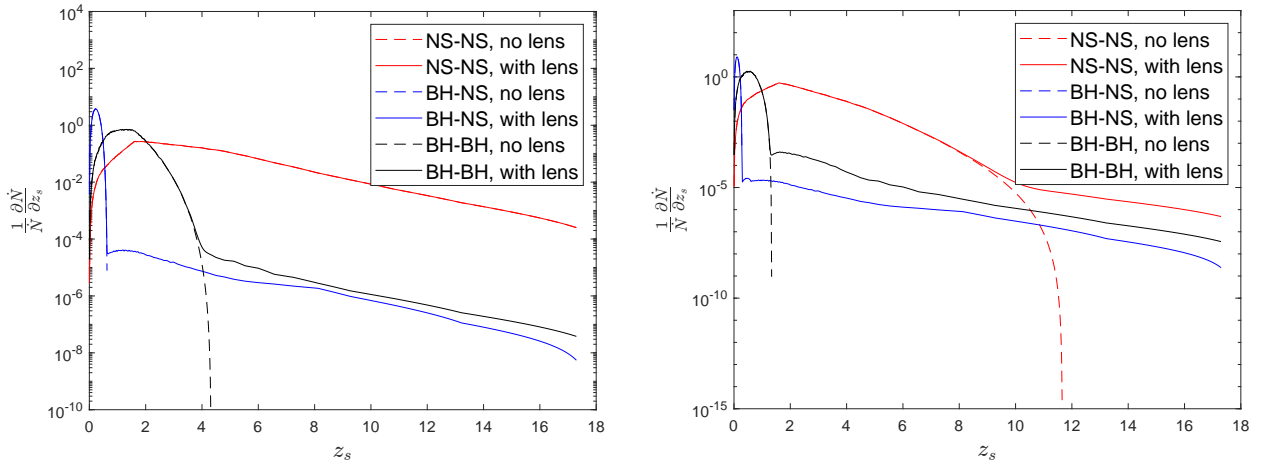


Figure 6. Probability densities of DCO inspiral events yearly rate to be detected by DECIGO (left panel) and B-DECIGO (right panel) during their survey duty cycles $T_{survey} = 4$ years. The solid curves are for the total catalogue of lensed and non-lensed systems, and the dashed curves are for the non-lensed ones. Note the logarithmic scale used in this figure.

shown. Detector's operation period of $T_{surv} = 4$ years is assumed. From these figures, one infers that the faint sources can be used to probe higher redshifts, and these higher redshift sources would thus contaminate the future catalog of gravitationally lensed GW events. This is expected on the ground of general idea of how the magnification bias works. Since DECIGO's characteristic radius r_0 is much larger than that of B-DECIGO, the former configuration is more suitable to probe high redshift sources, as shown by Fig. 5.

Besides the magnification bias on the lensed GW events, the magnification bias at the level of the full DCO inspiral events catalogue can also be obtained. For this end, one may calculate the detection rate of the intrinsically faint events whose I_+ image is magnified above the threshold. Table 5 shows the predictions for DECIGO and B-DECIGO. One can clearly see the increase in the detection rates, since $y_{+,max} > y_{-,max}$. Comparing this table with Table 2, one finds out that the magnification bias at the level of the resolvable inspiral DECIGO or B-DECIGO event catalogs would be of the order of $10^{-3} - 10^{-4}$ depending on the DCO population. This means that the cosmological inferences drawn from this catalog would not be affected very much.

One can demonstrate this effect by plotting together probability density of yearly detection rate of non-lensed sources and total prediction, which is shown in Fig. 6 for DECIGO and B-DECIGO. The upper panel of Fig. 6 shows that the magnification bias is negligible for all three types of the DCO sources in the case of DECIGO. For B-DECIGO, the magnification bias is negligibly small for NS-NS and BH-NS binaries, while for BH-BH binaries, it is barely noticeable, according to the lower panel of Fig. 6.

REFERENCES

- Abbott, B. P., et al. (The LIGO Scientific Collaboration and the Virgo Collaboration), 2016, PRL, 116, 061102
- Abbott, B. P., et al. (The LIGO Scientific Collaboration and the Virgo Collaboration), 2017a, PRL, 119, 161101
- Abbott, B. P., et al. (The LIGO Scientific Collaboration and Virgo Collaboration, FermiGamma-ray Burst Monitor, and INTEGRAL) 2017b, ApJL, 848, L13
- Abbott, B. P., et al. (The LIGO Scientific Collaboration and the Virgo Collaboration), 2019a, PRX, 9, 031040
- Abbott, B. P., et al. (The LIGO Scientific Collaboration and the Virgo Collaboration), 2019b, PRD, 100, 104036
- Abbott, B. P., et al. (The LIGO Scientific Collaboration and the Virgo Collaboration), 2020a, ApJL, 892, L3
- Abbott, B. P., et al. (The LIGO Scientific Collaboration and the Virgo Collaboration), 2020b, ApJL, 896, L44
- Amaro-Seoane, P., et al. 2017, arXiv:1702.00786
- Armano, M., et al. 2016, PRL, 116, 231101
- Belczyński, K., Kalogera, V., Bulik, T. 2002, ApJ, 572, 407
- Biesiada, M., Ding, X., Piórkowska, A., Zhu, Z.-H. 2014, JCAP, 10, 080
- Cao, S., Pan, Y., Biesiada, M., Godłowski, W., & Zhu, Z.-H. 2012, JCAP, 03, 016
- Cao, S., Covone, G., & Zhu, Z.-H. 2012, ApJ, 755, 31
- Cao, S., Biesiada, M., Gavazzi, R., Piórkowska, A., & Zhu, Z.-H. 2015, ApJ, 806, 185
- Cao, S., et al. 2019, NatSR, 9, 11608
- Cao, Z., Li, L.-F., Wang, Y. 2014, PRD, 90, 062003
- Choi, Y.-Y., Park, C., & Vogeley, M. S., 2007, ApJ, 658, 884
- Collett, T. E., Bacon, D. 2017, PRL, 118, 091101
- Coulter, D. A., et al. 2017, Science, 358, 1556
- Dai, L., Venumadhav, T., Sigurdson, K. 2017, PRD, 95, 044011
- Ding, X., Biesiada, M., & Zhu, Z.-H. 2015, JCAP, 12, 006
- Dominik, M., et al. 2012, ApJ, 759, 52
- Dominik, M., et al. 2013, ApJ, 779, 72
- Fan, X.-L., Liao, K., Biesiada, M., Piórkowska-Kurpas, A., & Zhu, Z.-H. 2017, PRL, 118, 091102
- Finn, L. S. 1996, PRD, 53, 2878
- Goldstein, A., et al. 2017, ApJL, 848, L14
- Hou, S., Li, P., Yu, H., Biesiada, M., Fan, X.-L., Kawamura, S., Zhu, Z.-H., "Lensing rates of gravitational wave signals displaying beat patterns detectable by DECIGO and B-DECIGO" 2020, PRD accepted [arXiv:2009.08116]
- Isoyama, S., Nakano, H., Nakamura T. 2018, Prog. Theor. Exp. Phys. 073E01
- Kawamura, S., et al. 2019, IJMPD, 28, 1845001
- Koopmans, L. V. E., et al. 2009, ApJL, 703, L51
- Li, S. S., Mao, S., Zhao, Y., & Lu, Y. 2018, MNRAS, 476, 2220
- Liao K., Fan X.-L., Ding X.-H., Biesiada M., Zhu Z.-H. 2017, Nat. Commun., 8, 1148
- Liao, K., Ding, X., Biesiada, M., Fan, X.-L., Zhu, Z.-H. 2018, ApJ, 867, 69
- Liao, K., Biesiada, M., & Fan, X.-L. 2019, ApJ, 875, 139
- Nakamura, T. 1998, PRL, 80, 1138
- Nakamura T., et al. 2016, Prog. Theor. Exp. Phys. 093E01 [arXiv:1607.00897]
- Ng, K. K. Y., Wong, K. W. K., Broadhurst, T., & Li, T. G. F. 2018, PRD, 97, 023012
- Oguri, M. 2018, MNRAS, 480, 3842
- Phinney, E. S. 2001, arXiv:0108028
- Piórkowska, A., Biesiada, M., Zhu, Z.-H. 2013, JCAP, 10, 022
- Sato S., et al. 2017, J. Phys.: Conf. Ser. 840, 012010
- Sereno, M., Sesana, A., Bleuler, A., Jetzer, P., Volonteri, M., & Begelman, M. C. 2010, PRL, 105, 251101
- Sereno, M., Jetzer, P., Sesana, A., & Volonteri, M. 2011, MNRAS, 415, 2773
- Seto, N., Kawamura, S., & Nakamura, T. 2001, PRL, 87, 221103
- Hou, S., Fan, X.-L., Liao, L., & Z. H. Zhu, 2020, PRD, 101, 064011
- Takahashi, R. & Nakamura, T. 2003, ApJ, 595, 1039
- Taylor, S. R. & Gair, J. R. 2012, PRD, 86, 023502
- Wei, J.-J. & Wu, X.-F. 2017, MNRAS, 472, 2906
- Yagi, K. & Seto, N. 2011, PRD, 83, 044011
- Yagi, K. 2013, IJMPD, 22, 1341013
- Yang, L., Ding, X., Biesiada, M., Liao, K., Zhu, Z.-H. 2019, ApJ, 874, 139
- Zhu, Z.-H. & Wu, X.-P. 1997, A&A, 324, 483
- Zhu, Z.-H. 1998, A&A, 338, 777